Impacts of climate and vegetation on actual evapotranspiration in typical arid mountainous regions using a Budyko-based framework

Yuanhui Yu, Yuyan Zhou, Weihua Xiao, Benqing Ruan, Fan Lu, Baodeng Hou, Yicheng Wang and Hao Cui

ABSTRACT

It is important to understand how actual evapotranspiration (ET_a) changes occur and what the dominant contributing factors are. This study investigated the impacts of climatic factor and vegetation coverage on the variations of ET_a using a Budyko-based framework. Climatic seasonal index and vegetation coverage index were selected as indicating factors. Two reservoir watersheds, i.e. the Wangkuai Reservoir Watershed and the Xidayang Reservoir Watershed, of the Daqing River Basin were selected as case studies. Also, relationships between the ET_a and climatic and vegetation factors were analyzed. Results showed that the improved vegetation conditions positively contributed to the ET_a changes, leading to an increase of 42.15 and 58.56 mm of ET_a in the two watersheds, while the increasing climate seasonality had a negative effect, resulting in a drop of 11.48 and 13.47 mm of ET_a. Vegetation coverage was recognized as the dominant factor to the changes of ET_a, compared to the climatic factor. Our research could offer supporting information for water resources management, agricultural production improvement and eco-environment construction in arid regions.

Key words | actual evapotranspiration, attribution, Budyko framework, climatic factor, vegetation coverage

Yuanhui Yu
Yuyan Zhou (corresponding author)
Weihua Xiao
Benqing Ruan
Fan Lu
Baodeng Hou
Yicheng Wang
Hao Cui
State Key Laboratory of Simulation and Regulation of Water Cycle in River Basin,
China Institute of Water Resources and Hydropower Research,
Beijing 100038,
China
E-mail: *zhouyuyan1@126.com*

Yuanhui Yu
Tsinghua University,
Beijing 100084,
China

HIGHLIGHTS

- This study investigated the impacts of climatic factor and vegetation coverage on the variations of actual evapotranspiration using a Budyko-based framework.
- The water-heat coupling controlling parameter of the Budyko-based framework was quantified by fitting the simulated actual evapotranspiration to observed actual evapotranspiration in a semi-empirical formula.

INTRODUCTION

Evapotranspiration (ET) is a crucial component in hydrological processes, which could account for up to over 60% of the precipitation on a global scale (Oki & Kanae 2006) and more than 90% in arid regions (Glenn *et al.* 2007). Given that the differences between precipitation and evapotranspiration (ET) have been commonly used to evaluate the water availability at catchment scale (Falkenmark *et al.* 1989), it is of vital importance to quantify the actual

doi: 10.2166/nh.2020.051

evapotranspiration (ET_a) and its influencing factors to assist decision making in water resources management and ecological protection.

Although it is often difficult to measure the ET_a directly either at field scale or at catchment scale, several ET_a quantification methods have been proposed including meteorological (Penman 1948; Bouchet 1963; Monteith 1965; Priestley & Taylor 1972; Allen *et al.* 1998), water balance (Liu 2018; Rodell *et al.* 2004, 2011; Zeng *et al.* 2013), energy balance and remote sensing techniques (Menenti & Choudhury 1993; Bastiaanssen *et al.* 1998; Su 2002). Particularly, the Food and Agriculture Organization (FAO) Penman–Monteith method has been globally recommended to estimate the crop reference ET (ET_0) (Allen *et al.* 1998). Based on the results of ET_0, the ET_a could therefore be estimated by multiplying the ET_0 by an empirical crop coefficient K_c (Allen *et al.* 1998; Xu *et al.* 2006; Drexler *et al.* 2008; Zhan *et al.* 2012; Yang *et al.* 2017). When there are a lack of crop coefficients in determining the ET_a, especially in mountainous regions where K_c is likely hard to be obtained (Drexler *et al.* 2008; Reddy 2015; Yang *et al.* 2017; Wang *et al.* 2019), development of the remote sensing-based evapotranspiration datasets provides a proxy in interpreting the spatiotemporal characteristics of the ET_a at catchment scale (Mauser & Schädlich 1998; Golubev *et al.* 2001; Xu *et al.* 2006; Bai & Liu 2018; Lu *et al.* 2019). These datasets are generated based on the implementation of remote sensing techniques in simulating the variation of ET, e.g. the MOD16 global evapotranspiration (ET) datasets (hereafter: the MODIS ET) (Cleugh *et al.* 2007; Mu *et al.* 2007, 2009, 2011), the Global Land Evaporation Amsterdam Model (GLEAM) datasets (hereafter: the GLEAM ET) (Miralles *et al.* 2011; Martens *et al.* 2017), the CSIRO PML ET (Commonwealth Scientific and Industrial Research Organisation Penman–Monteith–Leuning ET) data collection (Zhang *et al.* 2016) and the TerraClimate ET (Abatzoglou *et al.* 2018). For example, Tang & Zhang (2011) evaluated the performances of the MODIS ET in estimating the daily variation of ET in the Yellow River Basin. Li *et al.* (2017) applied the MODIS ET and another two ET products in capturing interannual variation of ET_a in the middle Yellow River Basin. Yang *et al.* (2018) quantified the spatiotemporal characteristics using the GLEAM ET over 10 basins in China.

It has been widely accepted that evapotranspiration (ET) changes with climate variability (Brümmer *et al.* 2012; Feng *et al.* 2013, 2020; Christoffersen *et al.* 2014; Beaulieu *et al.* 2016) and underlying surface conditions, particularly vegetation conditions (Donohue *et al.* 2007; Huo *et al.* 2013). As the only link between water and energy, ET is significantly affected by climate, in drought periods, temperature and sunshine hours had positive effects on the variation of ET, while other key climatic factors (i.e. effective precipitation, vapour pressure, wind speed, relative humidity) had negative effects on ET (Feng *et al.* 2013). As the global climate becomes warmer and warmer, it is generally expected that the evaporation will increase (Roderick & Farquhar 2002). Goyal (2004) suggested an increase of 14.8% of total ET demand with an increase in temperature by 20%. Xu *et al.* (2018) suggested that air temperature was one of the main climatic factors affecting ET_a trends, on the annual scale, as the temperature increases, ET_a decreases in the upper reaches of the Yellow River Basin. However, even as increasing air temperature has been observed over the last few decades, the evaporation could show a downward trend, known as the 'evaporation paradox' phenomenon (Peterson *et al.* 1995; Brutsaert & Parlange 1998; Roderick & Farquhar 2002). Feng *et al.* (2020) indicated that the dominant factor of ET variability varied with timescales and dry-wet conditions, and the precipitation plays a dominant role in ET variability in most arid regions. Brümmer *et al.* (2012) found that as the precipitation increased, ET tended to be stabilized. Yang *et al.* (2003) found that in arid and semi-arid regions of China, both precipitation and evaporation are decreasing, but the precipitation decreases faster than evaporation. ET_a was influenced by the vegetation greening degree, which is manifested in the increase in evaporation caused by vegetation coverage, and vice versa (Beaulieu *et al.* 2016). In arid areas, Bai *et al.* (2019) found that the inter-annual change of ET_a was driven by the NDVI (i.e. Normalized Difference Vegetation Index) with a contribution rate of 93%. He *et al.* (2019) found that the average impacts of vegetation restoration on ET change was 26.9% in the Loess Plateau, China. However, impacts of climate and vegetation on the variation of the ET_a have not reached a consensus.

According to the Budyko hypothesis, water and energy supply conditions (represented by precipitation and

potential evapotranspiration, respectively) are the two main factors controlling the actual evapotranspiration in the basin (Xu & Singh 2005), and are widely used in the study of evapotranspiration in the basin due to their concise expression and clear physical meaning. The Budyko framework provides a simple first-order relationship to estimate water availability represented by the ratio E/P as a function of the aridity index (Ep = P, with Ep denoting potential evaporation). The Budyko method is widely used in analyzing climate and vegetation factors, including arid regions and mountainous areas. Previous studies focus on the influence of ET in arid regions with a long series of climatic changes, while others focus on the influence of climatic extremes on ET in arid regions. However, there are few studies on the influence of vegetation and seasonal climatic changes on ET. Greve *et al.* (2016) proposed an analytically derived modification of the Budyko framework, that explicitly accounts for conditions under which ET is also driven by other water sources than precipitation (i.e. changes in water storage). Ning *et al.* (2018) employed four Budyko-based methods, namely the total differential method, complementary method, extrapolation method, and decomposition method, to attribute the changes in actual evapotranspiration in 13 basins in China's Loess Plateau. The results found that parameter ω was well-correlated with vegetation coverage and climate seasonality, and if the impacts of climate seasonality on ET were ignored, the contribution of vegetation will be estimated with a large error. Gao *et al.* (2017) used the Budyko framework to simulate the actual water consumption of 161 sub-basins from 1990 to 2014. The study indicates that with the vegetation recovery, the percentage of ET in the total precipitation keeps decreasing. However, at present, in arid mountainous regions research on these coefficients and parameters is still limited. It should be noted that large differences still exist in these studies, especially in quantifying the impacts of climate factors and vegetation conditions on ET_a. Particularly, in arid mountainous regions, there is still an urgent need to conduct further studies on the application of the Budyko method in revealing the climate-vegetation-hydrology interactions.

The objectives of this study were to investigate impacts of climatic factors and vegetation conditions on the variations of ET_a. Firstly, we quantify the changes of the climatic factors and vegetation conditions using ground-based and satellite-based observation data. Variations of the ET_a were validated by applying a Budyko-based empirical formula, which was fitted by the data of climatic factors and vegetation conditions. The water-heat coupling control parameter ω was therefore quantified according to the empirical formula. Based on the above results, we made an attribution analysis on the variation of ET_a to the climatic factors and vegetation coverage by applying a total differential method. Case studies are conducted in two reservoir watersheds in the Daqing River Basin (DRB), which act as two of the most important water supply regions in this river basin. It is interesting to note that the Xiong'an New Area, which depends largely on these two watersheds in the river basin, has received widespread attention from the scientific community, leading to an emerging focus on the hydrological processes and attribution anlaysis in this region.

METHODOLOGY

Study area

We selected the Wangkuai Reservoir Watershed (WRW) and Xidayang Reservoir Watershed (XRW) as the study area, which are two typical arid mountainous regions located in the DRB, North China. These two watersheds act as the main water storage in the river basin and provide more than 80% of water resources to downstream of the DRB. These two watersheds are of great significance as the two reservoirs are two of the multiple water sources of the Xiong'an New Area, which faces large challenges in guaranteeing its water security in the coming future. The geophysical location of the study area is shown in Figure 1. The two watersheds are located between 113°40′–115°E and 38°30′ ~ 39°45′N in the mountainous region of DRB, where the vegetation coverage area accounts for more than 70% of the watersheds. Mountains and plains characterize the topography of DRB. The northwest is mainly composed of mountainous areas, the middle region is a plain area, and the eastern low-lying area is the Baiyangdian Lake area. This region has a semi humid continental monsoon climate.

The areas of WRW and XRW are 3,662 and 1,296 km^2, respectively. The average annual precipitation of WRW is

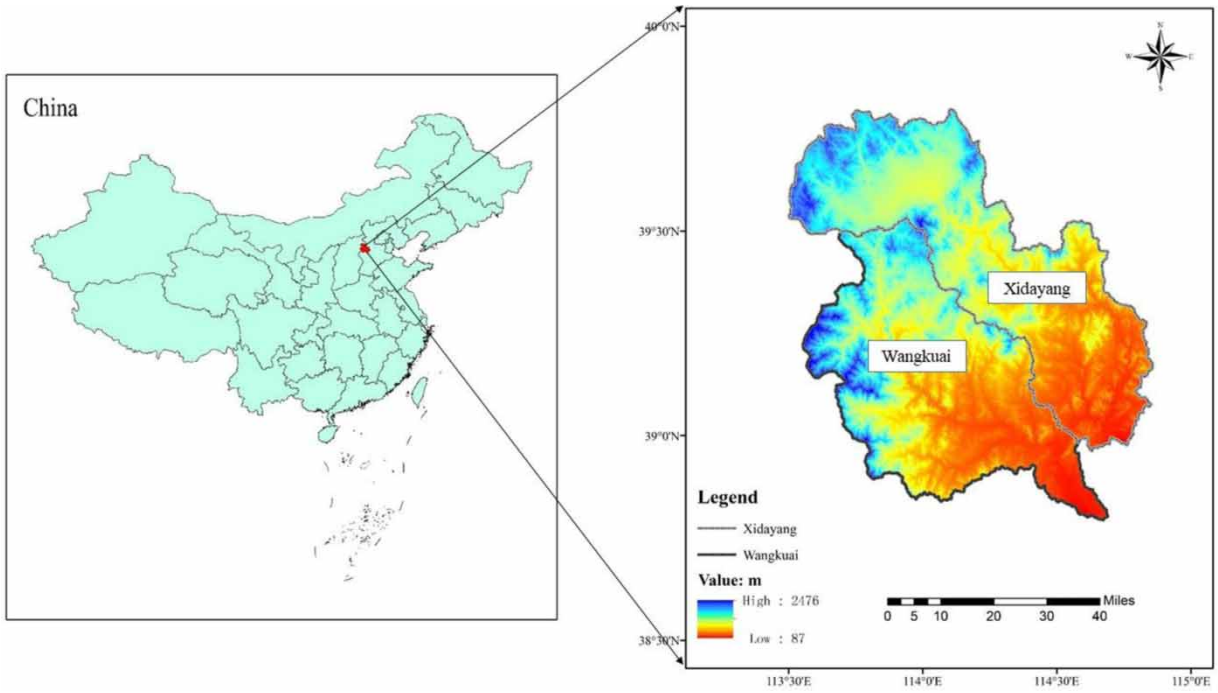

Figure 1 | The location of Wangkuai Reservoir Watershed and Xidayang Reservoir Watershed.

about 416 mm, while it is about 394 mm in XRW. The average outbound flow of WRW is 240 million m³, and that of XRW is 130 million m³.

Data

Meteorological data

Daily meteorological data for the period 1961–2018, including precipitation, temperature, sunshine hours and relative humidity, were obtained from the China Meteorological Administration (CMA, http://data.cma.cn/). Digital elevation data, at 30 m resolution, was provided by the Geospatial Data Cloud site, Computer Network Information Centre, Chinese Academy of Sciences (www.gscloud.cn/).

Vegetation data

In this study, MODIS satellite remote sensing data MOD13A2 were selected to analyze the NDVI variations characteristics in the DRB (Daqing River Basin). The MOD13A2 product provides Vegetation Index (VI) values at a per pixel basis at 1 km spatial resolution. It contains the NDVI, which is referred to as the continuity index to the existing National Oceanic and Atmospheric Administration-Advanced Very High-Resolution Radiometer (NOAA-AVHRR) derived NDVI. The algorithm for this product chooses the best available pixel value from all the acquisitions from the 16-day period (Holben 1986). The criteria used is low clouds, low view angle and the highest NDVI value. The MODIS product NDVI data from 2000 to 2015 were obtained and used to estimate the dynamic of vegetation activity in the DRB. Data is obtained from geospatial data cloud sites (www.gscloud.cn/).

Evapotranspiration data

In this study, MODIS satellite remote sensing data MOD16A2 were obtained and used to analyze the actual evapotranspiration from 2000 to 2015 in the DRB. Provided in the MOD16A2 product are layers for composited evapotranspiration (ET), latent heat flux (LE), potential ET (PET) and potential LE (PLE) along with a quality control layer. The pixel values for the two evapotranspiration layers (ET and PET) are the sum of all 8 days within the composite period and the pixel values for the two latent heat layers

(LE and PLE) are the average of all 8 days within the composite period. ET was extracted for analysis of actual evapotranspiration in this paper. The datasets were 500 m resolution and 8-day evapotranspiration products. Data was obtained from the net of EarthData (https://ladsweb.modaps.eosdis.nasa.gov).

Methods

The Budyko function

The Budyko framework can take a number of mathematical forms. In this study, Fu's function (Fu 1981) was used to assess the impacts of climatic and vegetation factors on ET_a. This function was selected for its simple structure and clear physical meaning with few parameters applied:

$$\frac{ET}{P} = 1 + \frac{ET_p}{P} - \left[1 + \left(\frac{ET_p}{P}\right)^{\omega}\right]^{1/\omega}$$

$$\frac{ET}{ET_p} = 1 + \frac{P}{ET_p} - \left[1 + \left(\frac{P}{ET_p}\right)^{\omega}\right]^{1/\omega} \quad (1)$$

where P is precipitation; ET_p is potential evapotranspiration calculated using the method of Priestley & Taylor (1972); ω is the water-heat coupling control parameter which is a parameter that represents the vegetation and topography of the river basin, and its value range is [1, $+\infty$]. The changes in water storage were often ignored at annual scale (Zhao *et al.* 2011).

Indices for vegetation and climatic factors

Vegetation coverage index (M) was chosen to represent the catchment vegetation condition and was estimated following Yang *et al.* (2009):

$$M = \frac{NDVI - NDVI_{min}}{NDVI_{max} - NDVI_{min}} \quad (2)$$

where $NDVI_{max}$ and $NDVI_{min}$ are NDVI values for dense forest and bare soil, respectively. The range of M is between 0 and 1. The larger M is, the more the vegetation cover there is.

The climate seasonality index (S), proposed by Milly (1994) and Woods (2003), has been widely used to reflect the seasonal variations between P and ET_0 (Yang *et al.* 2012; Abatzoglou & Ficklin 2017; Ning *et al.* 2017). It can be expressed as:

$$S = |\delta_P - \delta_{ET_0} \varnothing| \quad (3)$$

where $\varnothing$ is the dryness index, $\varnothing = \overline{ET_0}/\bar{P}$. δ_P and δ_{ET_0} are the seasonal amplitudes of P and ET_0, respectively. They represent the range of precipitation and potential evapotranspiration. S reflects the non-uniformity in the intra-annual distribution of water and energy (Ning *et al.* 2017).

According to Fu's formula, when $\omega \to 1$, $ET \to 0$. Therefore, the values of M and S are: when $ET \to 0$, vegetation transpiration $T \to 0$, that is, $M \to 0$. Or when runoff $R \to P$, the matching between precipitation and potential evapotranspiration tends to be the worst, that is, $S \to \infty$.

According to the relationship between ω, M and S under extreme conditions, that is, boundary conditions (Ning *et al.* 2019):

$$f_1(M) \to 0,\ i.e.,\ \omega \to 1,\ when\ M \to 0;$$

$$f_2(S) \to 0,\ i.e.,\ \omega \to 1,\ when\ S \to \infty.$$

The general form of parameter can be expressed as follows:

$$\omega = 1 + a \times M^b \times exp(cS) \quad (4)$$

where a, b and c are constants.

In order to verify the performances of the empirical formula, we tested the above formulas by estimating the annual ET of the two watersheds against the MODIS ET measurements combining with the Fu's function (Zhang *et al.* 2004).

Attribution analysis to climate and vegetation factors

In order to fully understand the contribution of climatic and vegetation variables to ET changes, contribution analysis was applied in our study. The total differential method is one of the most widely used methods in the attribution of water cycle change. Since ω is the hydrothermal coupling

parameter, the contribution of M and S to ET_a can be calculated by using Fu's function with the total differential method. The total differential method is actually Taylor's first-order expansion. Based on the complementary relation of elasticity coefficient (Zhou *et al.* 2015), the following equation is proposed:

$$\frac{\partial ET/ET}{\partial P/P} + \frac{\partial ET/ET}{\partial ET_p/ET_p} = 1$$

Based on algebraic identity derivation, a method for attributing evapotranspiration (runoff) change is proposed:

$$\begin{aligned}\Delta ET =& \alpha\left[\left(\frac{\partial ET}{\partial P}\right)_1 \Delta P + \left(\frac{\partial ET}{\partial ET_p}\right)_1 \Delta ET_p + P_2\Delta\left(\frac{\partial ET}{\partial P}\right)\right. \\ &\left. + ET_{p,2}\Delta\left(\frac{\partial ET}{\partial ET_p}\right)\right] + (1-\alpha)\left[\left(\frac{\partial ET}{\partial P}\right)_2 \Delta P\right. \\ &\left. + \left(\frac{\partial ET}{\partial ET_p}\right)_2 \Delta ET_p + P_1\Delta\left(\frac{\partial ET}{\partial P}\right) + ET_{p,1}\Delta\left(\frac{\partial ET}{\partial ET_p}\right)\right]\end{aligned}$$

α is the weight coefficient and its value range is [0, 1]. In this paper, 0.5 as recommended by Zhou *et al.* (2015) is adopted.

By using the total differential method applied in Zhou *et al.* (2015), this method can accurately decompose the variation of hydrology change into two parts, therefore separating the contribution of climate change and the contribution of water-heat coupling control parameter ω changes. The contribution of precipitation, potential evapotranspiration (ET_p) and water-heat coupling control parameter ω can be expressed as:

$$C(P) = \alpha\left[\left(\frac{\partial ET}{\partial P}\right)_1 \Delta P\right] + (1-\alpha)\left[\left(\frac{\partial ET}{\partial P}\right)_2 \Delta P\right] \quad (5)$$

$$C(ET_p) = \alpha\left[\left(\frac{\partial ET}{\partial ET_p}\right)_1 \Delta ET_p\right] + (1-\alpha)\left[\left(\frac{\partial ET}{\partial ET_p}\right)_2 \Delta ET_p\right] \quad (6)$$

$$\begin{aligned}C(\omega) =& \alpha\left[P_2\Delta\left(\frac{\partial ET}{\partial P}\right)_1 + ET_{p,2}\Delta\left(\frac{\partial ET}{\partial ET_p}\right)\right] \\ &+ (1-\alpha)\left[P_1\Delta\left(\frac{\partial ET}{\partial P}\right) + ET_{p,1}\Delta\left(\frac{\partial ET}{\partial ET_p}\right)\right]\end{aligned} \quad (7)$$

where α is the weight coefficient, and the value range is [0,1]. The value of α is recommended to be equal to 0.5 in this study.

The semi-empirical formula is used to distinguish the contribution of M and S, after obtaining the relative contributions (RC) of M and S to the change of ω, the contributions of M and S to ET change can be expressed as:

$$C(M) = C(\omega) * RC(M) \quad (8)$$

$$C(S) = C(\omega) * RC(S) \quad (9)$$

$RC(M)$ and $RC(S)$ represent the contribution rate of vegetation coverage and climate seasonal index to ET change, which can be calculated by the following formula:

$$RC(x) = \frac{C_x}{L_{ET}} \times 100\%$$

C_x represents the contribution of meteorological factors to ET change. L_{ET} represents the change of ET on the multi-year scale, mm/yr. In order to simplify the calculation process, the contribution can be approximately calculated by multiple linear regression method.

Statistical methods

The moving average method was used to test the variations trend of meteorological data and NDVI sequence, and the Mann–Kendall method was used to test the significance of the trend ($p \leq 0.05$). Analysis of variance (ANOVA) was used for the difference test of M and S. The linear correlation method was used to analyze the correlation between vegetation and climate seasonality factors to ET_a.

In this study, mean absolute error (MAE), the square root of the mean square error (RMSE) and Nash–Sutcliffe coefficient of efficiency (NSE) were selected to describe the deviation between estimated ET_a and measured ET_a by the water-heat coupling control parameter ω.

$$MAE = \frac{\sum_{i=1}^{n} |ET_{estimated,i} - ET_{measured,i}|}{n} \quad (10)$$

$$RMSE = \sqrt{\frac{\sum_{i=1}^{n} (ET_{estimated,i} - ET_{measured,i})^2}{n}} \quad (11)$$

$$NSE = 1 - \frac{\sum_{i=1}^{n} (ET_{estimated,i} - ET_{measured,i})^2}{\sum_{i=1}^{n} (ET_{measured,i} - \overline{ET_{measured}})^2} \quad (12)$$

where i represents the time series, n represents the length of the time period, and $ET_{estimated,i}$ and $ET_{measured,i}$ represent the estimated and measured values of the actual evapotranspiration of a basin in a certain year.

RESULTS

Quantification of the climatic and vegetation indices

The annual temperature and precipitation of WRW and XRW showed a rising trend (Figure 2).

Similar increasing trends are witnessed in the two watersheds in terms of the vegetation coverage index (M), with the mean M value of the WRW and XRW being 0.49 and 0.45. The slope of M is 0.01 in both WRW and XRW, and the fluctuation is similar. (Table 1 and Figure 3(a)). The vegetation index changes from 0.41 to 0.54 in the past 16 years for the WRW, while the index varies from 0.37 to 0.51 for the XRW. Significant increasing trends are observed for these two watersheds from 2000 to 2015 ($p < 0.05$) (Table 1 and Figure 3(a)). It can be seen from the ANOVA analysis results that significant differences have been found between the variations of the vegetation cover trends ($p < 0.05$, F > F-crit, Table 1).

In terms of the climate seasonality index (S), it is shown that a contradictory trend has been found in the two watersheds. In WRW and XRW, the slope of S is 0.02 and –0.001 respectively (Figure 3(b)). For the WRW, the S tends to show an overall upward trend, ranging from 0.06 to 0.90 with a mean value of 0.49. Large annual variations are found in the WRW, the maximum differs from the minimum by 0.85 (Figure 3(b)), while a slight drop of the S in the XRW is shown, ranging from 0.02 to 0.19. Fewer annual variations exist compared with those of the WRW. It should be noted

Table 1 | Variations of the M and S values and statistics results

		Statistics		ANOVA analysis		
Index	Watersheds	Mean value	Range	*p*-value	F	F-crit
M	WRW	0.49	0.41–0.54	0.01	7.17	4.17
	XRW	0.45	0.37–0.51			
S	WRW	0.49	0.06–0.90	5.5×10^{-7}	40.11	4.17
	XRW	0.10	0.02–0.19			

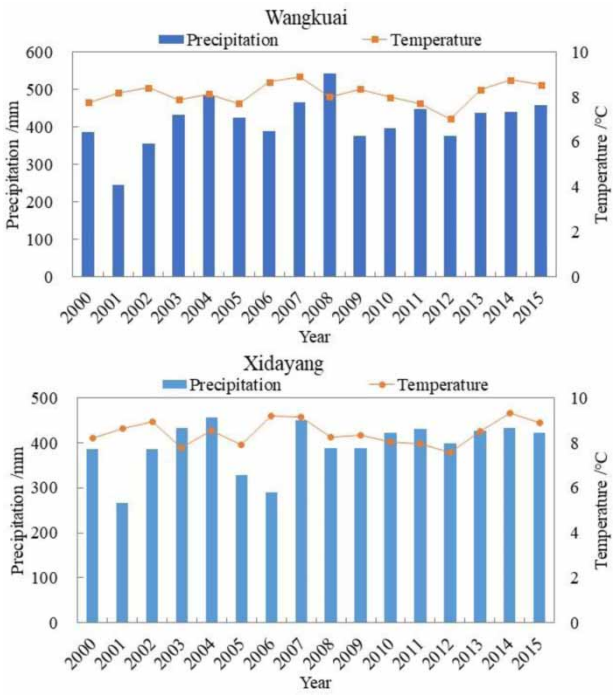

Figure 2 | Temperature and precipitation changes of WRW and XRW from 2000 to 2015.

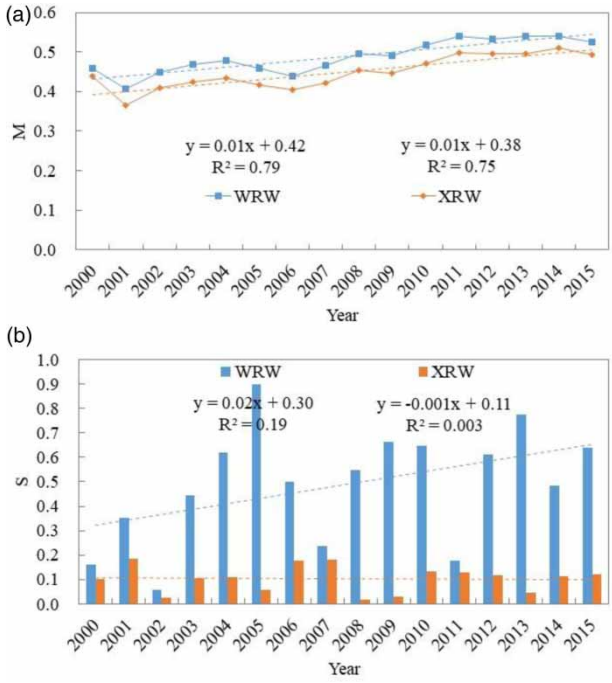

Figure 3 | Variation trends of vegetation coverage M and climate seasonal index S in WRW and XRW from 2000 to 2015.

that large significant difference between the S values of the two watersheds have been found ($p < 0.01$, F > F-crit) (Table 1).

Validation of the estimated ET_a

Based on the Budyko framework, the relationships between the water-heat coupling control parameter ω and the vegetation coverage index M and the climate seasonality index S are examined using the least linear square regression method. The regression formulas are shown as follows:

$$\text{WRW:}\quad \omega = 1 + 15.89 \times M^{1.875} \times exp(-5.627 \cdot S) \quad (R^2 = 0.47) \tag{13}$$

$$\text{XRW:}\quad \omega = 1 + 0.897 \times M^{-0.76} \times exp(-0.864 \cdot S) \quad (R^2 = 0.43) \tag{14}$$

These formulas are verified by comparing the estimated ET by Fu's equation and measured ET from the MODIS ET data. The verification results showed that both the formulas could estimate the ET_a well at annual scale, with a low value of MAE and RMSE and good performances in terms of NSE (Table 2 and Figure 4). There are many methods to estimate ET, among which the Romanenko (Rom1, Rom2) (Romanenko 1961) and Penman method simplified by Linacre (L-P) (Linacre 1977) have been widely applied. We estimated the variations of ET by Rom1, Rom2 and L-P. The correlation coefficient R^2 of the three methods in WRW were 0.69, 0.65 and 0.67, and in XRW were 0.81, 0.72 and 0.80. Although the overall fitting effect of these methods was good, the accuracy of ET_a is less than that of Fu's method (Table 3). Therefore, we deduce that Fu's method could be more applicable in estimating actual evapotranspiration in this study.

Table 2 | The accuracy verification results of estimation of annual ET in watershed by the parameter ω semi-empirical formula

	ET estimate precision /mm		
Watershed	**MAE**	**RMSE**	**NSE**
WRW	-2.5×10^{-5}	8.5×10^{-5}	1
XRW	0.81	3.22	0.99

Attribution of ET_a variations to climatic and vegetation factors

The results showed that the ET_a presented a significant increasing trend in the two watersheds based on the MODIS ET data (Figure 5). The ET_a of these two watersheds

Table 3 | Correlation coefficient R^2 of different methods for evapotranspiration estimation

Watershed	Rom1	Rom2	L-P	Fu
WRW	0.69	0.65	0.67	1
XRW	0.81	0.72	0.80	0.99

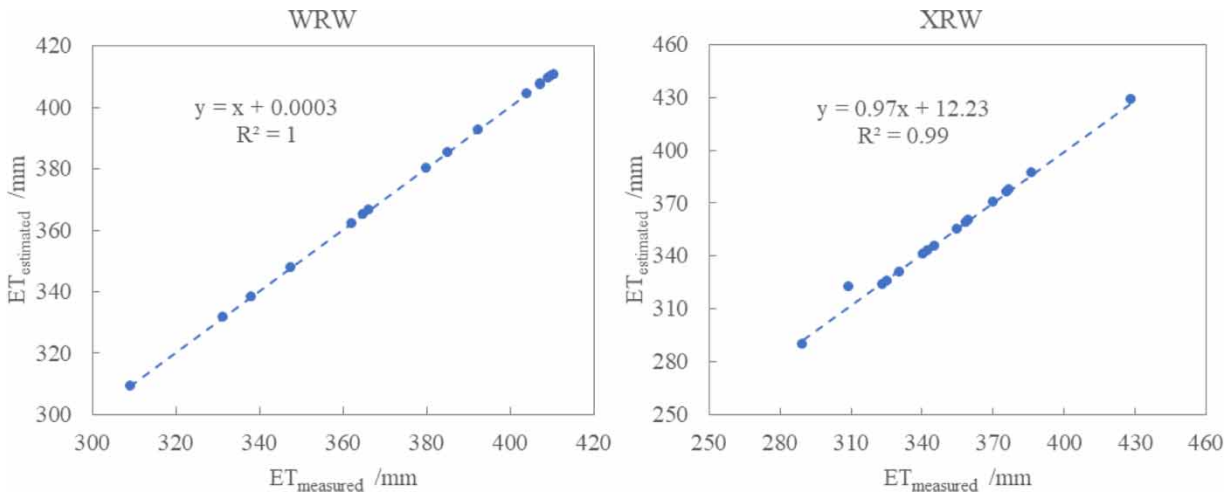

Figure 4 | Comparison of averaged annual ET estimates derived using Equations (13) and (14).

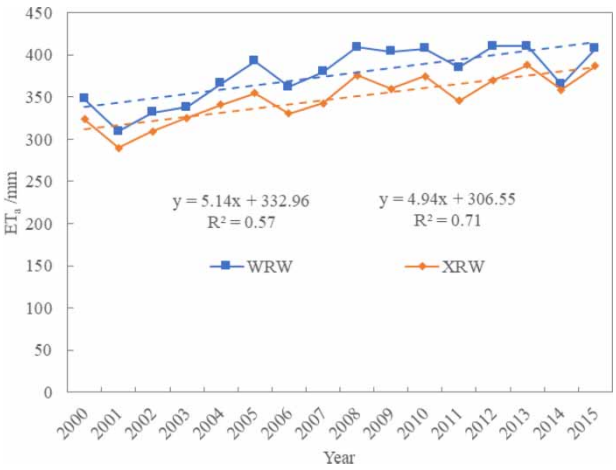

Figure 5 | ET changes of WRW and XRW from 2000 to 2015.

rises swiftly from 289 to 415 mm within 16 years, with a mean value of 388.94 and 360.41 mm for the WRW and XRW, respectively. In this study, we attempted to determine the effects of vegetation and climatic index on the annual variation of ET_a in the two watersheds via attribution analysis.

The correlation analysis shows that the ET_a increases with the rising of vegetation coverage at annual scale (Figure 6). Significant positive correlation has been found between the variation of ET_a and the vegetation index (M) in these two watersheds (Figure 6). However, no significant linear relationships exist between ET_a and the climate seasonality index (S) (Figure 7). Particularly, the climate seasonality index is positively related with the ET_a in the WRW, while a negative relationship is found in the XRW. These results indicated that the variation of vegetation coverage may exert a consistent effect on the variation of ET_a, while the effects of climatic factor may change across watersheds (Zhang *et al.* 2001; Donohue *et al.* 2007, 2010).

We also investigate the contribution of variation of climate and vegetation factors to the changes of ET_a by applying a total difference method. Results showed that the vegetation index explained up to 42.15–58.56 mm of the variations of the ET_a in the two watersheds, which is determined as the main influencing factor to the change. However, the climate seasonality index tends to lead to a decreasing trend of ET_a in the two watersheds, with negative contribution rates of 11.48 and 13.47 mm, respectively (Table 4).

According to the results analysis of the contribution, the contribution of precipitation is second only to vegetation (Table 4). The precipitation is more sensitive than other climate factors in this area (Figure 8).

DISCUSSION

Attribution of actual evapotranspiration in arid regions

In this study we used the observed meteorological data from two reservoir watersheds in DRB. Additionally, we applied the data of climate factor and vegetation coverage to analyze the variation of ET_a in WRW and XRW of DRB. The results

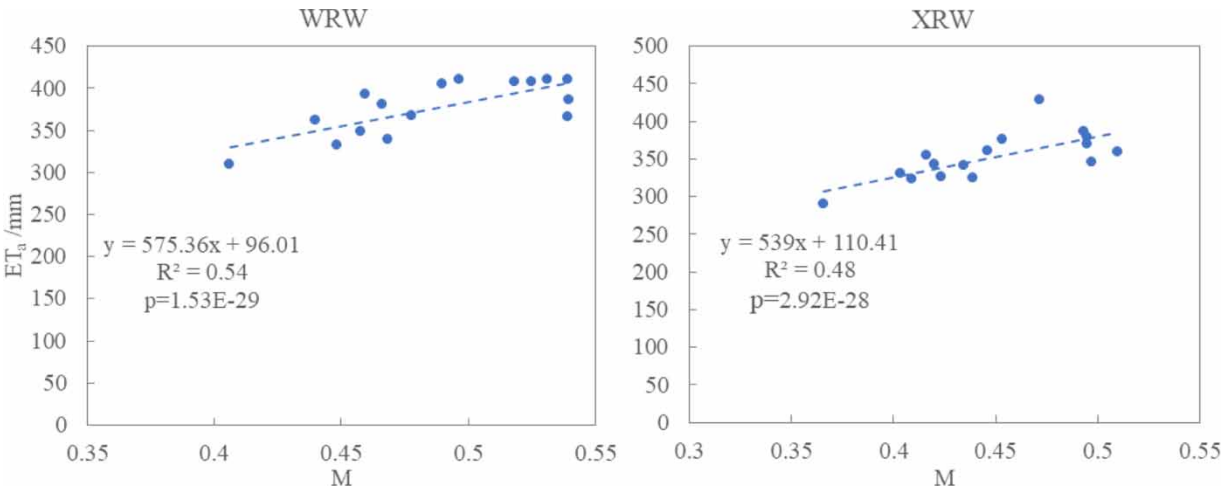

Figure 6 | Relationship between annual ET and vegetation coverage M in WRW and XRW.

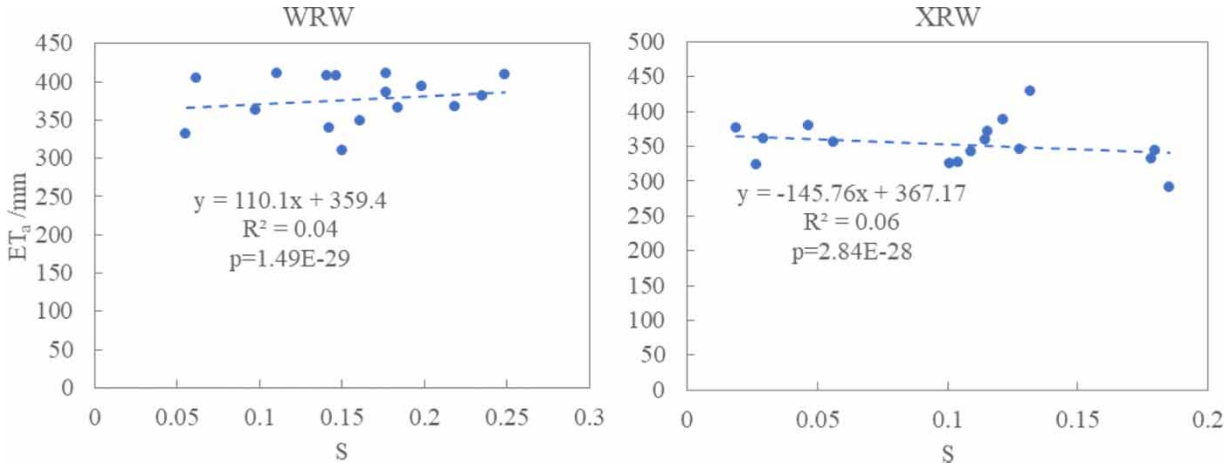

Figure 7 | Relationship between annual ET and climate seasonal index S in WRW and XRW.

Table 4 | The correlation coefficient and contribution of each influence factor changes to ET in WRW and XRW

Watershed	R^2 (ET-M)	R^2 (ET-S)	C(P)/mm	C(ω)/mm	C(M)/mm	C(S)/mm
WRW	0.56	0.04	15.61	30.68	42.15	−11.48
XRW	0.53	0.07	15.55	45.09	58.56	−13.47

showed that there was a larger correlation between vegetation factors and ET_a, and the contribution of climate factors was slightly less than that of vegetation factors. We deduced that the vegetation factor is likely to be the main contributing factor to the variations of ET_a.

There have been many methods for the quantitative attribution study of evapotranspiration time change, such as linear multiple regression (Shan *et al.* 2015), detrending method (Xu *et al.* 2006) and sensitivity analysis (Wang *et al.* 2013). However, the research on the spatial variation attribution of evapotranspiration is mostly in the qualitative description stage (Li *et al.* 2012; Zhang *et al.* 2015). The Budyko method considers the effects of vegetation, topography and meteorological factors on evapotranspiration, which is conducive to a more detailed study. The above findings are generally consistent with previous studies on the ET_a attribution analysis across arid regions. For example, Ning *et al.* (2020) found that vegetation coverage averaged across all the catchments has increased obviously, and has further led to the increase in ET_a in China, especially in the dry catchments, while the variation amplitude of precipitation was small. Liu *et al.* (2019b) found that greening was the major reason for the ET_a increases in the Ziya-Daqing Basins, which are partially included in the mountainous regions of the Haihe River Basin. Xu *et al.* (2018) found that large-scale coherent vegetation greening would be the primary factor affecting inter-annual ET_a in comparison with climate factors in the upper reaches of the Yellow River Basin. Ma *et al.* (2019) found that vegetation greening was the dominant factor to the increases of ET_a in mixed forest and grassland in the Loess Plateau. In these studies, we found that the variation amplitudes of their vegetation were larger than those of precipitation and temperature. Moreover, compared with the correlation between precipitation and temperature on ET_a, vegetation has a greater correlation with ET_a. Particularly, in the Daqing River Basin where the two reservoir watersheds are located, Cui *et al.* (2019) revealed that there exists a significant increasing trend of vegetation coverage, especially in the mountainous regions. This may serve as an important reason for the increase of ET_a in the DRB. Recent studies have attempted to elaborate the mechanism of vegetation and ET_a interactions in arid regions. Findings of these studies indicate that the greening of vegetation could lead to the rising of ET_a in a number of patterns, e.g. increasing the water storage in the watersheds and reducing runoff to downstreams (Chang *et al.* 2017). Experimental studies like Feng *et al.* (2016) and Jaramillo *et al.* (2018) deduced that the changing of the leaf stomatal conductance, surface roughness and leaf area index and biomass of trees under the greening circumstance could substantially influence ET_a.

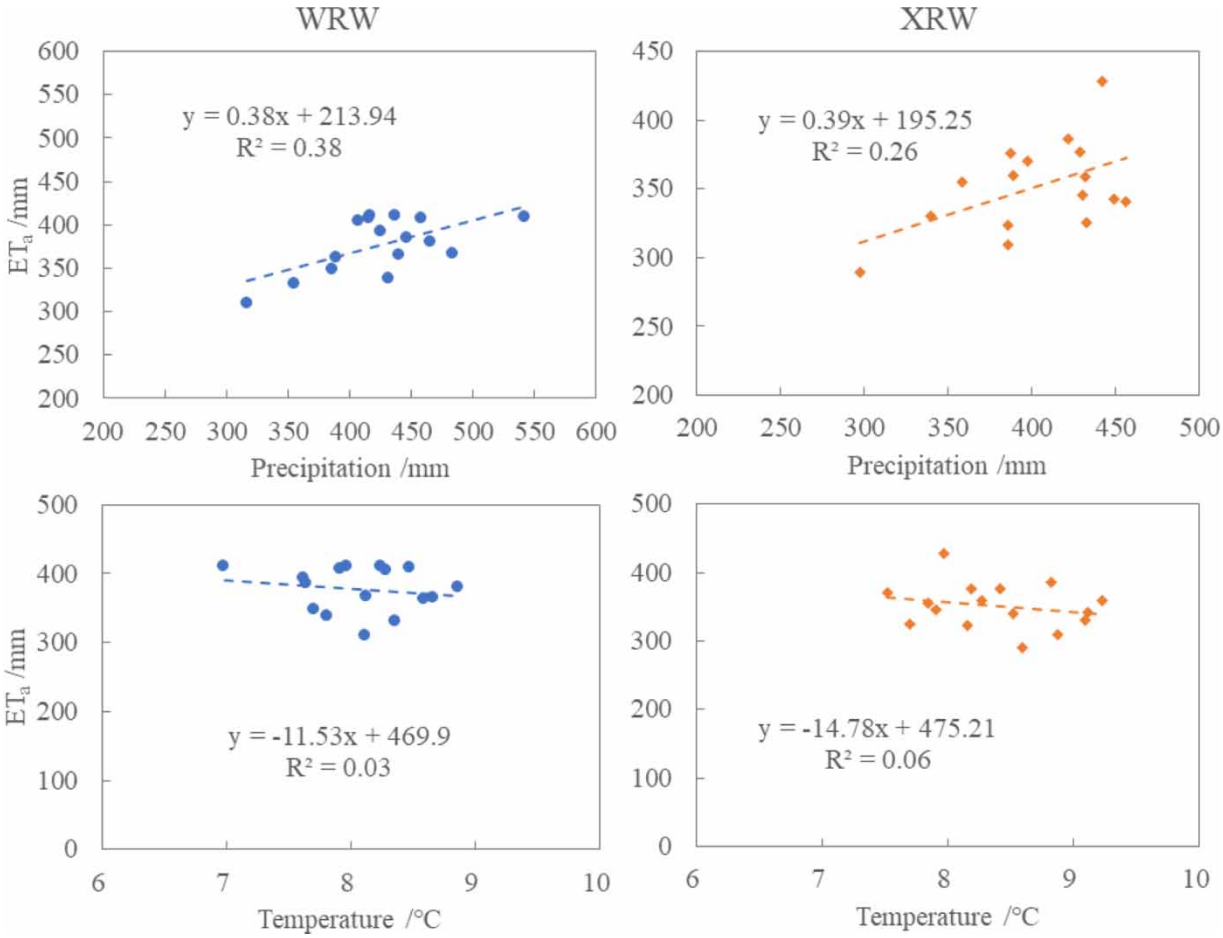

Figure 8 | Relationships between annual ET and precipitation, temperature in WRW and XRW.

Some studies, however, have come to the opposite conclusion. For example, Feng *et al.* (2020) indicated that precipitation plays a dominant role in ET_a variability in most arid regions. This may due to the large variability of precipitation and the small variability of vegetation in these regions. Particularly, in arid regions such as Xinjiang Province in Northwest China and the Loess Plateau, the large precipitation amplitude is the main controlling factor affecting ET_a. He *et al.* (2019) found that the variations of precipitation contributed the largest proportion of the ET_a changes in the Loess Plateau, where significant fluctuations of annual precipitation were observed in the study area. However, a recent study by Ning *et al.* (2017) is basically consistent with the conclusion of our results, indicating that vegetation, rather than precipitation, is the leading factor of the variations of ET_a via a comparative study in 13 watersheds in arid areas of Northern China. Therefore, we deduce that it is of great necessity to incorporate the variations of climatic factors, e.g. precipitation, and vegetation coverage in arid regions into the attribution analysis of the ET_a.

Implications of the variation and attribution of the ET_a in mountainous regions

Two reservoir watersheds in mountainous regions of the DRB are selected as case studies. Mountain regions are experiencing more pronounced climate change than other global land areas. Xu *et al.* (2020) indicate that vegetation greening and/or earlier growing season are imposing positive effects on evapotranspiration in mountainous areas. In this study, climate and vegetation factors affecting actual evapotranspiration in two major reservoirs of the DRB

were analyzed, and attribution analysis was conducted using the Budyko framework, which has guiding significance for water resources regulation and management, agricultural production and ecological construction in the basin. Similar results are found in the mountainous regions of the North China Plain, one of the most severe water scarce regions in the world. The results indicated that the improved vegetation conditions could positively contribute to the ET_a changes. For example, Liu *et al.* (2019a) found that crop coefficients (K_c) and leaf area index (LAI) were positively correlated with ET_a in the North China Plain. Wu & Xing (2016) pointed out that the change of ET_a in Haihe River Basin was positively correlated with the change of vegetation cover area. Cao *et al.* (2018) found that vegetation change had a promoting effect on ET_a, the increase of forest area enhanced the evapotranspiration capacity of the basin in the Chaohe Basin of the North China Plain. In other mountainous areas, e.g. the Loess Plateau, climate change has been reported to have significant impacts on the hydrological processes. Nevertheless, changes of vegetation could also exert great impacts on the variations of ET_a. For instance, Xu *et al.* (2018) quantified the sensitivity of climate and vegetation growth changes to ET_a in the upper reaches of the Yellow River Basin, revealing that both the regional averaged NDVI and ET_a showed an increasing trend, where positive relationships were detected between these two variables. Ma *et al.* (2019) reported that under the circumstance of ecological restoration in the Loess Plateau, recovering vegetation has affected the ET_a in the past 16 years significantly.

Uncertainty

There are certain uncertainties in our study, which may come from the uncertainty of methods, data and parameters. We use the total differential method for attribution analysis under the Budyko framework. The partial derivative coefficients in the total differential method should be calculated by the complete Taylor expansion method so as to obtain accurate results. However, in our study, the partial derivative coefficient is estimated as a first-order approximation. Yang *et al.* (2014) showed that ignoring the higher-order coefficients of the Taylor expansion would lead to an underestimation of the contribution of climate change to hydrological processes as precipitation increases. And since the R^2 of the semi-empirical formula is less than 0.5, the change of vegetation coverage M and climate seasonal index S cannot fully explain the interannual variation of parameter ω. In this study, we used MODIS datasets to analyze the actual evapotranspiration. Results showed that ET_a data of MODIS is slightly higher than the ground-based observed data. This may lead to a higher value for the study of the contribution of vegetation coverage to ET_a. Since the difference between MODIS-ET_a and ground-based observed ET_a is very small and the linear fitting result is very good, the error between MODIS-ET_a and ground-based observed ET_a can be ignored. The relationships of parameter ω with vegetation coverage and climate seasonality index in the two watersheds were not significant in this study (Figure 9). This implies that ω might represent the combined effects of some other factors. For example, strong interactions among vegetation, climate, and soil conditions will lead to specific hydrologic partitioning at the catchment scale (Ning *et al.* 2017).

The possibility of other impact factors

This study focused on the impacts of climatic factors and vegetation coverage on ET_a, particularly in arid mountainous regions. Nevertheless, there may be other factors affecting ET_a, such as human activities, irrigation and water use, which may not be quantified by the Budyko-based framework in one study. Liu *et al.* (2019b) investigated the attribution of evapotranspiration changes in the west area of China and found that human activities (e.g. air pollution, urbanization, and water supply project) may be one factor to influence ET_a. Sun & Ren (2013) found that ET_a from irrigated farmland increased in Haihe River Basin, and land use played the dominant role in the ET_a changes. Djaman *et al.* (2016) pointed out that crop water use efficiency is related to ET_a and irrigation water demand, and ET_a is positively correlated with irrigation. Jung *et al.* (2010) found that the decrease of the annual ET_a from 1998 to 2008 resulted from the decrease of the soil moisture in many regions of the world. Further studies are warranted in quantifying the impacts of other factors, e.g. human activities, construction and regulation of water supply infrastructures, on the variations of ET_a in these regions.

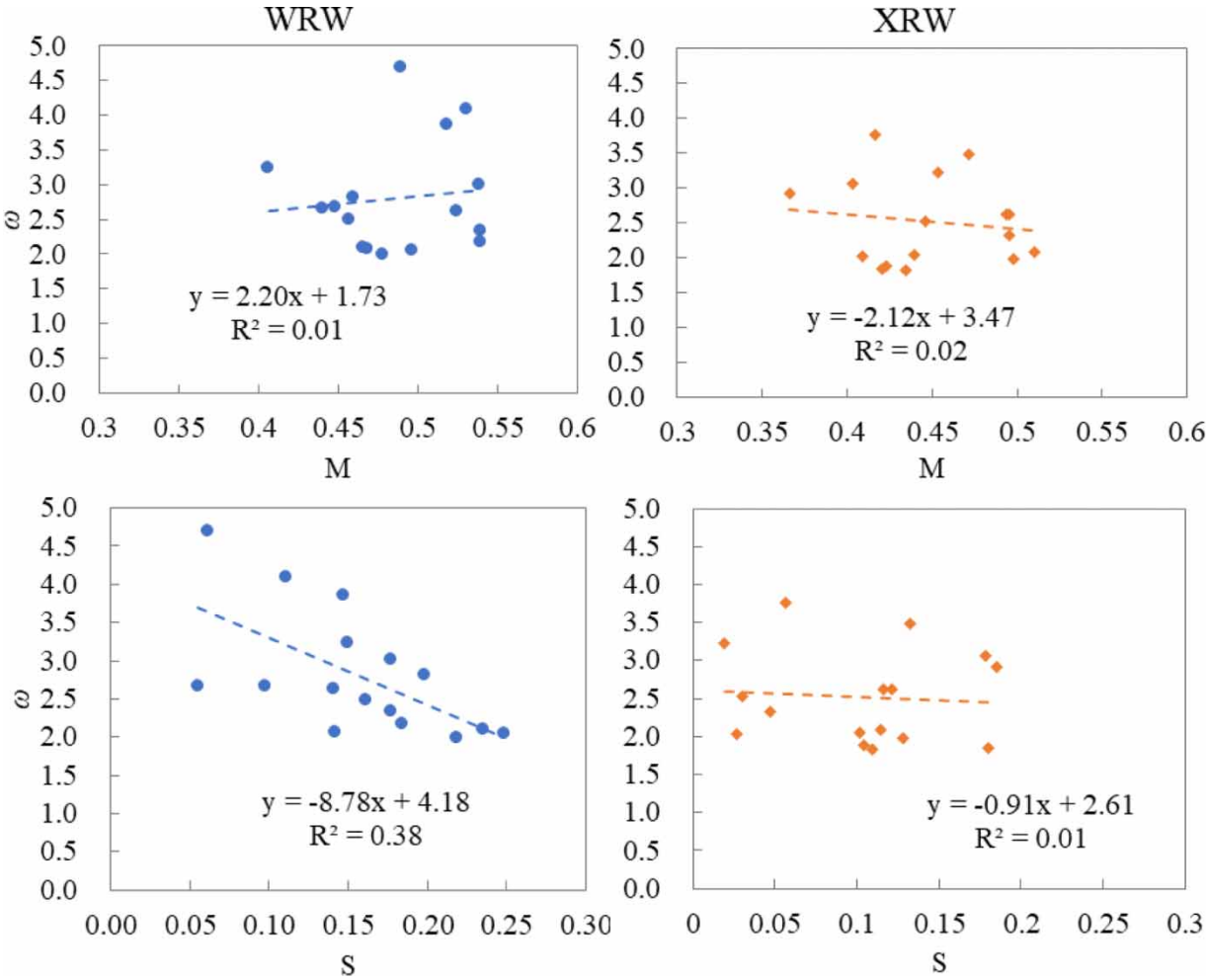

Figure 9 | Relationship between ω and vegetation coverage (M) and climate seasonality index (S) in the WRW and XRW.

CONCLUSIONS

This study, using a Budyko-based framework, explored the impacts of climate and vegetation on actual evapotranspiration typical arid mountainous regions. This study quantified the climatic and vegetation indices, validated the accuracy of the estimated ET_a, and researched the attribution of ET_a variations to climatic and vegetation factors. The conclusions can be summarized as follows:

(1) The increase of vegetation coverage led to the increase of ET_a in arid mountainous river basins such as the upper reservoir watersheds of the Daqing River Basin.
(2) In arid mountainous regions, vegetation coverage may be the main impact factor relative to climate factors, especially for regions with large change of vegetation coverage but little change of climate factors. The contributions of vegetation were 42.15 and 58.56 mm, and that of climate factor were −11.48 and −13.47 mm, in the WRW and XRW, respectively.

The actual evapotranspiration ET_a in the study area showed an increasing trend from 2000 to 2015, and the vegetation cover also showed a green trend. The increase of vegetation led to the increase of evapotranspiration, which had a negative impact on the water resources and water supply in the downstream. Therefore, the extent of vegetation restoration in the upstream needed to be limited. Moreover, a proxy strategy is to choose crops that use less water and are suitable for growing in arid regions. Findings

of this study tend to be a reference in exploring the complex climate-vegetation-hydrology relationships in arid mountainous regions.

ACKNOWLEDGEMENTS

This work was jointly supported by the National Key Research and Development Program of China (Grant No. 2018YFC0406506 and 2018YFC0406501), the National Natural Science Foundation of China (No. 51909275 and 51779271) and Guangxi Graduate Education Innovation Project (YCBZ2018023).

DATA AVAILABILITY STATEMENT

All relevant data are included in the paper or its Supplementary Information.

REFERENCES

Abatzoglou, J. T. & Ficklin, D. L. 2017 Climatic and physiographic controls of spatial variability in surface water balance over the contiguous United States using the Budyko relationship. *Water Resources Research* **53**, 7630–7643.

Abatzoglou, J. T., Dobrowski, S. Z., Parks, S. A. & Hegewisch, K. C. 2018 Terraclimate, a high-resolution global dataset of monthly climate and climatic water balance from 1958–2015. *Scientific Data* **5**, 1–12.

Allen, R. G., Pereira, L. S., Raes, D. & Smith, M. 1998 *Crop Evapotranspiration – Guidelines for Computing Crop Water Requirements*. FAO Irrigation and Drainage Paper 56. FAO, Rome, Italy.

Bai, P. & Liu, X. 2018 Intercomparison and evaluation of three global high-resolution evapotranspiration products across China. *Journal of Hydrology* **566**, 743–755.

Bai, M., Mo, X., Liu, S. & Hu, S. 2019 Contributions of climate change and vegetation greening to evapotranspiration trend in a typical hilly-gully basin on the Loess Plateau, China. *Science of the Total Environment* **657**, 325–339.

Bastiaanssen, W. G. M., Menenti, M., Feddes, R. A. & Holtslag, A. A. M. 1998 A remote sensing surface energy balance algorithm for land (SEBAL). 1. Formulation. *Journal of Hydrology* **212–213**, 198–212.

Beaulieu, E., Lucas, Y., Viville, D., Chabaux, F. O., Ackerer, P., Goddéris, Y. & Pierret, M.-C. 2016 Hydrological and vegetation response to climate change in a forested mountainous catchment. *Modeling Earth Systems and Environment* **2**, 191–205.

Bouchet, R. J. 1963 *Evapotranspiration Réelle et Potentielle, Signification Climatique (Real and Potential Evapotranspiration Climate Meaning)*. In: *General Assembly of Berkeley, 19–31 August 1963: Committee for Evaporation*. International Association of Hydrological Sciences. IASH Publication, Wallingford, pp. 134–142.

Brümmer, C., Black, T. A., Jassal, R. S., Grant, N. J., Spittlehouse, D. L., Chen, B., Nesic, Z., Amiro, B. D., Arain, M. A., Barr, A. G., Bourque, C. P.-A., Coursolle, C., Dunn, A. L., Flanagan, L. B., Humphreys, E. R., Lafleur, P. M., Margolis, H. A., McCaughey, J. H. & Wofsy, S. C. 2012 How climate and vegetation type influence evapotranspiration and water use efficiency in Canadian forest, peatland and grassland ecosystems. *Agricultural and Forest Meteorology* **153**, 14–30.

Brutsaert, W. & Parlange, M. 1998 Hydrologic cycle explains the evaporation paradox. *Nature* **396**, 30.

Cao, W., Zhang, Z., Zha, T., Wang, S., Guo, J. & Xu, X. 2018 Exploring the effects of vegetation dynamics and climate changes on the Chaohe watershed actual evapotranspiration – Budyko Hypothesis approach. *Acta Ecologica Sinica* **38**, 5750–5758.

Chang, X., Zhao, W., Liu, B., Liu, H., He, Z. & Du, J. 2017 Can forest water yields be increased with increased precipitation in a Qinghai spruce forest in arid northwestern China? *Agricultural and Forest Meteorology* **247**, 139–150.

Christoffersen, B. O., Restrepo-Coupe, N., Arain, M. A., Baker, I. T., Cestaro, B. P., Ciais, P., Fisher, J. B., Galbraith, D., Guan, X., Gulden, L., Hurk, B. V. D., Ichii, K., Imbuzeiro, H., Jain, A., Levine, N., Miguez-Macho, G., Poulter, B., Roberti, D. R., Sakaguchi, K., Sahoo, A., Schaefer, K., Shi, M., Verbeeck, H., Yang, Z.-L., Araújo, A. C., Kruijt, B., Manzi, A. O., Rocha, H. R. D., Randow, C. V., Muza, M. N., Borak, J., Costa, M. H., Alves, L. G. G. A. D. G., Zeng, X. & Saleska, S. R. 2014 Mechanisms of water supply and vegetation demand govern the seasonality and magnitude of evapotranspiration in Amazonia and Cerrado. *Agricultural and Forest Meteorology* **191**, 33–50.

Cleugh, H. A., Leuning, R., Mu, Q. & Running, S. W. 2007 Regional evaporation from flux tower and MODIS satellite data. *Remote Sensing of Environment* **106**, 285–354.

Cui, H., Xiao, W., Zhou, Y., Hou, B., Lu, F. & Pei, M. 2019 Spatial and temporal variations of vegetation cover and responses to climatic variables in Daqing River Basin, North China. *Journal of Coastal Research* **93**, 450–459.

Djaman, K., Mel, V., Balde, A., Bado, V., Manneh, B., Diop, L., Mutiibwa, D., Rudnick, D., Irmak, S. & Futakuchi, K. 2016 Evapotranspiration, irrigation water requirement and water productivity of rice (*Oryza sativa* L.) in the Sahelian environment. *Paddy and Water Environment* **15**, 469–482.

Donohue, R. J., Roderick, M. L. & McVicar, T. R. 2007 On the importance of including vegetation dynamics in Budyko's hydrological model. *Hydrology and Earth System Sciences* **11**, 983–995.

Donohue, R. J., Roderick, M. L. & McVicar, T. R. 2010 Can dynamic vegetation information improve the accuracy of Budyko's hydrological model? *Journal of Hydrology* **390**, 23–34.

Drexler, J. Z., Anderson, F. E. & Snyder, R. L. 2008 Evapotranspiration rates and crop coefficients for a restored marsh in the Sacramento–San Joaquin Delta, California, USA. *Hydrological Processes* **22**, 725–735.

Falkenmark, M., Lundqvist, J. & Widstrand, C. 1989 Macro-scale water scarcity requires micro-scale approaches. *Natural Resources Forum* **13**, 258–267.

Feng, J., Yan, D., Li, C., Yu, F. & Zhang, C. 2013 Assessing the impact of climatic factors on potential evapotranspiration in droughts in North China. *Quaternary International* **6**, 6–12.

Feng, X., Fu, B., Piao, S., Wang, S. & Ciais, P. 2016 Revegetation in China's Loess Plateau is approaching sustainable water resource limits. *Nature Climate Change* **6**, 1019–1022.

Feng, S., Liu, J., Zhang, Q., Zhang, Y., Singh, V. P., Gu, X. & Sun, P. 2020 A global quantitation of factors affecting evapotranspiration variability. *Journal of Hydrology* **12**, 135–146.

Fu, B. 1981 On the calculation of the evaporation from land surface (in Chinese). *Journal of Atmospheric Sciences* **5**, 23–31.

Gao, X., Sun, M., Zhao, Q., Wu, P., Zhao, X., Pan, W. & Wang, Y. 2017 Actual ET modelling based on the Budyko Framework and the sustainability of vegetation water use in the Loess Plateau. *Science of the Total Environment* **579**, 1550–1559.

Glenn, E. P., Huete, A. R., Nagler, P. L., Hirschboeck, K. K. & Brown, P. 2007 Integrating remote sensing and ground methods to estimate evapotranspiration. *Critical Reviews in Plant Sciences* **26**, 139–168.

Golubev, V. S., Lawrimore, J. H., Groisman, P. Y., Speranskaya, N. A., Zhuravin, S. A., Menne, M. J., Peterson, T. C., Thomas, C. & Malone, R. W. 2001 Evaporation changes over the contiguous united states and the former USSR: a reassessment. *Geophysical Research Letters* **28**, 2665–2668.

Goyal, R. K. 2004 Sensitivity of evapotranspiration to global warming: a case study of arid zone of Rajasthan (India). *Agricultural Water Management* **69**, 1–11.

Greve, P., Gudmundsson, L., Orlowsky, B. & Seneviratne, S. I. 2016 A two-parameter Budyko function to represent conditions under which evapotranspiration exceeds precipitation. *Hydrologic and Earth System Sciences* **20**, 2195–2205.

He, G., Zhao, Y., Wang, J., Gao, X., He, F., Li, H., Zhai, J., Wang, Q. & Zhu, Y. 2019 Attribution analysis based on Budyko hypothesis for land evapotranspiration change in the Loess Plateau, China. *Journal of Arid Land* **11** (6), 147–161.

Holben, B. N. 1986 Characteristics of maximum-value composite images from temporal Avhrr data. *International Journal of Remote Sensing* **7**, 1417–1434.

Huo, Z. L., Dai, X. Q., Feng, S. Y., Kang, S. Z. & Huang, G. H. 2013 Effect of climate change on reference evapotranspiration and aridity index in arid region of China. *Journal of Hydrology* **492**, 24–34.

Jaramillo, F., Cory, N., Arheimer, B., Laudon, H., van der Velde, Y., Hasper, T. B., Teutschbein, C. & Uddling, J. 2018 Dominant effect of increasing forest biomass on evapotranspiration: interpretations of movement in Budyko space. *Hydrology and Earth System Sciences* **22**, 567–580.

Jung, M., Reichstein, M., Ciais, P., Seneviratne, S. I., Sheffield, J., Goulden, M. L., Bonan, G., Cescatti, A., Chen, J., Jeu, R. D., Dolman, A. J., Eugster, W., Gerten, D., Gianelle, D., Gobron, N., Heinke, J., Kimball, J., Law, B. E., Montagnani, L., Mu, Q., Mueller, E., Oleson, K., Papale, D., Richardson, A. D., Roupsard, O., Running, S., Tomelleri, E., Viovy, N., Weber, U., Williams, C., Wood, E., Zaehle, S. & Zhang, K. 2010 Recent decline in the global land evapotranspiration trend due to limited moisture supply. *Nature* **467**, 951–954.

Li, Z., Zheng, F. L. & Liu, W. Z. 2012 Spatiotemporal characteristics of reference evapotranspiration during 1961–2009 and its projected changes during 2011–2099 on the Loess Plateau of China. *Agricultural and Forest Meteorology* **154**, 147–155.

Li, Y., Liang, K., Liu, C., Liu, W. & Bai, P. 2017 Evaluation of different evapotranspiration products in the middle Yellow River Basin, China. *Hydrology Research* **48**, 498–513.

Linacre, E. T. 1977 A simple formula for estimating evaporation rates in various climates, using temperature data alone. *Agricultural Meteorology* **18**, 409–424.

Liu, W. 2018 Evaluating remotely sensed monthly evapotranspiration against water balance estimates at basin scale in the Tibetan Plateau. *Hydrology Research* **49**, 1977–1990.

Liu, Y., Chen, J. & Pan, T. 2019a Analysis of changes in reference evapotranspiration, pan evaporation, and actual evapotranspiration and their influencing factors in the North China Plain during 1998–2005. *Earth and Space Science* **6**, 1366–1377.

Liu, Y., Mo, X., Hu, S., Chen, X. & Liu, S. 2019b Attribution analyses of evapotranspiration and gross primary productivity changes in Ziya-Daqing basins, China during 2001–2015. *Theoretical and Applied Climatology* **15**, 1175–1189.

Lu, Z., Zhao, Y., Wei, Y., Feng, Q. & Xie, J. 2019 Differences among evapotranspiration products affect water resources and ecosystem management in an Australian catchment. *Remote Sensing* **11**, 958–975.

Ma, Z., Yan, N., Wu, B., Stein, A., Zhu, W. & Zeng, H. 2019 Variation in actual evapotranspiration following changes in climate and vegetation cover during an ecological restoration period (2000–2015) in the Loess Plateau, China. *Science of the Total Environment* **689**, 689–700.

Martens, B., Miralles, D. G., Lievens, H., van der Schalie, R., de Jeu, R. A. M., Fernández-Prieto, D., Beck, H. E., Dorigo, W. A. & Verhoest, N. E. C. 2017 GLEAM v3: satellite-based land evaporation and root-zone soil moisture. *Geoscientific Model Development* **10**, 1903–1925.

Mauser, W. & Schädlich, S. 1998 Modelling the spatial distribution of evapotranspiration on different scales using remote sensing data. *Journal of Hydrology* **212–213**, 250–267.

Menenti, M. & Choudhury, B. 1993 Parameterization of land surface evaporation by means of location dependent potential evaporation and surface temperature range. In: *Exchange Processes at the Land Surface for a Range of Space and Time Scales* (H. J. Bolle, ed.). IAHS Publication, Wallingford, pp. 561–568.

Milly, P. C. D. 1994 Climate, soil-water storage, and the average annual water-balance. *Water Resources Research* **30**, 2143–2156.

Miralles, D. G., Holmes, T. R. H., De Jeu, R. A. M., Gash, J. H., Meesters, A. G. C. A. & Dolman, A. J. 2011 Global land-surface evaporation estimated from satellite-based observations. *Hydrology and Earth System Sciences* **15**, 453–469.

Monteith, J. L. 1965 Evaporation and environment. *Symposia of the Society for Experimental Biology* **19**, 205–234.

Mu, Q., Heinsch, F. A., Zhao, M. & Running, S. W. 2007 Development of a global evapotranspiration algorithm based on MODIS and global meteorology data. *Remote Sensing of Environment* **111**, 519–536.

Mu, Q., Jones, L. A., Kimball, J. S., McDonald, K. C. & Running, S. W. 2009 Satellite assessment of land surface evapotranspiration for the pan-Arctic domain. *Water Resources Research* **45**, 94–113.

Mu, Q., Zhao, M. & Running, S. W. 2011 Improvements to a MODIS global terrestrial evapotranspiration algorithm. *Remote Sensing of Environment* **115**, 1781–1800.

Ning, T., Li, Z. & Liu, W. 2017 Vegetation dynamics and climate seasonality jointly control the interannual catchment water balance in the Loess Plateau under the Budyko framework. *Hydrology and Earth System Sciences* **21**, 1–25.

Ning, T., Li, Z., Feng, Q., Liu, W. & Li, Z. 2018 Comparison of the effectiveness of four Budyko-based methods in attributing long-term changes in actual evapotranspiration. *Scientific Reports* **10**, 1–10.

Ning, T., Zhou, S., Chang, F., Shen, H., Li, Z. & Liu, W. 2019 Interaction of vegetation, climate and topography on evapotranspiration modelling at different time scales within the Budyko framework. *Agricultural and Forest Meteorology* **275**, 59–68.

Ning, T., Li, Z., Feng, Q., Chen, W. & Li, Z. 2020 Effects of forest cover change on catchment evapotranspiration variation in China. *Hydrological Processes* **10**, 2219–2228.

Oki, T. & Kanae, S. 2006 Global hydrological cycles and world water resources. *Science* **313**, 1068–1072.

Penman, H. L. 1948 Natural evaporation from open water, bare soil and grass. *Proceedings of the Royal Society of London. Series A, Mathematical and Physical Sciences* **193**, 120–145.

Peterson, T. C., Golubev, V. S. & Groisman, P. Y. 1995 Evaporation losing its strength. *Nature* **377**, 687–688.

Priestley, C. & Taylor, R. 1972 On the assessment of surface heat flux and evaporation using large-scale parameters. *Monthly Weather Review* **100**, 81–92.

Reddy, K. C. 2015 Development of crop coefficient models of castor and maize crops. *European Journal of Agronomy* **69**, 59–62.

Rodell, M., Famiglietti, J. S., Chen, J., Seneviratne, S. I., Viterbo, P., Holl, S. & Wilson, C. R. 2004 Basin scale estimates of evapotranspiration using GRACE and other observations. *Geophysical Research Letters* **31**, 1–4.

Rodell, M., McWilliams, E. B., Famiglietti, J. S., Beaudoing, H. K. & Nigro, J. 2011 Estimating evapotranspiration using an observation based terrestrial water budget. *Hydrological Processes* **25**, 4082–4092.

Roderick, M. L. & Farquhar, G. D. 2002 The cause of decreased pan evaporation over the past 50 years. *Science* **298**, 1410–1411.

Romanenko, V. A. 1961 Computation of the autumn soil moisture using a universal relationship for a large area. In *Proceedings Ukrainian Hydrometeorological Research Institute*, Kiev, Russia.

Shan, N., Shi, Z., Yang, X., Zhang, X., Guo, H., Zhang, B. & Zhang, Z. 2015 Trends in potential evapotranspiration from 1960 to 2013 for a desertification-prone region of China. *International Journal of Climatology* **36** (10), 3434–3445.

Su, Z. 2002 The Surface Energy Balance System (SEBS) for estimation of turbulent heat fluxes. *Hydrology and Earth System Sciences* **6**, 85–100.

Sun, C. & Ren, L. 2013 Assessment of surface water resources and evapotranspiration in the Haihe River basin of China using SWAT model. *Hydrological Processes* **27**, 1200–1222.

Tang, Q. & Zhang, X. 2011 Mapping evapotranspiration using MODIS and GRACE data. In *19th International Conference on Geoinformatics*. IEEE, Shanghai, China.

Wang, W., Xing, W., Shao, Q., Yu, Z., Peng, S., Yang, T., Yong, B., Taylor, J. & Singh, V. P. 2013 Changes in reference evapotranspiration across the Tibetan Plateau: observations and future projections based on statistical downscaling. *Journal of Geophysical Research* **118**, 4049–4068.

Wang, S., Zhui, G., Xia, D., Ma, J., Han, T., Ma, T., Zhang, K. & Shang, S. 2019 The characteristics of evapotranspiration and crop coefficients of an irrigated vineyard in arid Northwest China. *Agricultural Water Management* **212**, 388–398.

Woods, R. 2003 The relative roles of climate, soil, vegetation and topography in determining seasonal and long-term catchment dynamics. *Advances in Water Resources* **26**, 295–309.

Wu, R. & Xing, X. 2016 Variation characteristics and influencing factors of actual evapotranspiration under various vegetation types: a case study in the Huaihe River Basin, China. *Chinese Journal of Applied Ecology* **27**, 1727–1736.

Xu, C. Y. & Singh, V. P. 2005 Evaluation of three complementary relationship evapotranspiration models by water balance approach to estimate actual regional evapotranspiration in different climatic regions. *Journal of Hydrology* **308**, 105–121.

Xu, C.-Y., Gong, L., Jiang, T., Chen, D. & Singh, V. P. 2006 Analysis of spatial distribution and temporal trend of reference evapotranspiration and pan evaporation in Changjiang (Yangtze River) catchment. *Journal of Hydrology* **327**, 81–93.

Xu, S., Yu, Z., Yang, C., Ji, X. & Zhang, K. 2018 Trends in evapotranspiration and their responses to climate change and

vegetation greening over the upper reaches of the Yellow River Basin. *Agricultural and Forest Meteorology* **263**, 118–129.

Xu, S., Yu, Z., Lettenmaier, D., McVicar, T. & Ji, X. 2020 Elevation-dependent response of vegetation dynamics to climate change in a cold mountainous region. *Environmental Research Letters* **15**, 203–215.

Yang, J., Ding, Y., Chen, S. & Liu, L. 2003 Variations of precipitation and evaporation in North China in recent 40 years. *Journal of Arid Land Resources & Environment* **17**, 6–11.

Yang, D., Shao, W., Yeh, P. J. F., Yang, H., Kanae, S. & Oki, T. 2009 Impact of vegetation coverage on regional water balance in the nonhumid regions of China. *Water Resources Research* **45**, 507–519.

Yang, H., Lv, H., Yang, D. & Hu, Q. 2012 Seasonality of precipitation and potential evaporation and its impact on catchment water-energy balance (in Chinese). *Journal of Hydroelectric Engneering* **24**, 54–59.

Yang, H. B., Yang, D. W. & Hu, Q. F. 2014 An error analysis of the Budyko hypothesis for assessing the contribution of climate change to runoff. *Water Resources Research* **50**, 9620–9629.

Yang, Y., Chen, R., Song, Y., Han, C., Liu, J. & Liu, Z. 2017 Actual daily evapotranspiration and crop coefficients for an alpine meadow in the Qilian Mountains, northwest China. *Hydrology Research* **48**, 1131–1142.

Yang, X., Yong, B., Yin, Y. & Zhang, Y. 2018 Spatio-temporal changes in evapotranspiration over China using GLEAM_V3.0a products (1980–2014). *Hydrology Research* **49** (5), 1330–1348.

Zeng, Z., Wang, T., Zhou, F., Ciais, P., Mao, J., Shi, X. & Piao, S. 2013 A worldwide analysis of spatiotemporal changes in water balance-based evapotranspiration from 1982 to 2009. *Journal of Geophysical Research: Atmospheres* **119**, 1186–1202.

Zhan, F., Zhou, G., Wang, Y., Yang, F. & Nilsson, C. 2012 Evapotranspiration and crop coefficient for a temperate desert steppe ecosystem using eddy covariance in Inner Mongolia, China. *Hydrological Processes* **26**, 379–386.

Zhang, L., Dawes, W. R. & Walker, G. R. 2001 Response of mean annual evapotranspiration to vegetation changes at catchment scale. *Water Resources Research* **37**, 701–708.

Zhang, L., Hickel, K., Dawes, W. R., Chiew, F. H. S., Western, A. W. & Briggs, P. R. 2004 A rational function approach for estimating mean annual evapotranspiration. *Water Resources Research* **40**, 1–14.

Zhang, Q., Qi, T. Y., Li, J. F., Singh, V. P. & Wang, Z. Z. 2015 Spatiotemporal variations of pan evaporation in China during 1960–2005: changing patterns and causes. *International Journal of Climatology* **35**, 903–912.

Zhang, Y., Peña-Arancibia, J. L., McVicar, T. R., Chiew, F. H. S., Vaze, J., Liu, C., Lu, X., Zheng, H., Wang, Y., Liu, Y. Y., Miralles, D. G. & Pan, M. 2016 Multi-decadal trends in global terrestrial evapotranspiration and its components. *Science Reports* **6**, 1–12.

Zhao, Q. L., Liu, X. L., Ditmar, P., Siemes, C., Revtova, E., Hashemi-Farahani, H. & Klees, R. 2011 Water storage variations of the Yangtze, Yellow, and Zhujiang river basins derived from the DEOS mass transport (DMT-1) model. *Science China – Earth Sciences* **54**, 667.

Zhou, S., Yu, B., Huang, Y. & Wang, G. 2015 The complementary relationship and generation of the Budyko functions. *Geophysical Research Letters* **42**, 1781–1790.

First received 30 April 2020; accepted in revised form 12 November 2020. Available online 21 December 2020